Controlling fluid flows with positive polynomials

LASAGNA Davide[1], HUANG Deqing[2], TUTTY Owen R.[1], CHERNYSHENKO Sergei [3]

1. Engineering and the Environment, University of Southampton, Highfield, Southampton, SO17 1BJ, UK
E-mail: davide.lasagna@soton.ac.uk, o.r.tutty@soton.ac.uk

2. School of Electrical Engineering, Southwest Jiaotong University, Chengdu, 610031, China
E-mail: elehd2012@gmail.com

3. Department of Aeronautics, Imperial College London, Prince Consort Road, London SW7 2AZ, UK
E-mail: s.chernyshenko@imperial.ac.uk

Abstract: A novel nonlinear feedback control design methodology for incompressible fluid flows aiming at the optimisation of long-time averages of key flow quantities is presented. The key idea, first outlined in Ref. [1], is that the difficulties of treating and optimising long-time averages are relaxed by shifting the analysis to upper/lower bounds for minimisation/maximisation problems, respectively. In this setting, control design reduces to finding the polynomial-type state-feedback controller that optimises the bound, subject to a polynomial inequality constraint involving the cost function, the nonlinear system, the controller itself and a tunable polynomial function. A numerically tractable approach, based on Sum-of-Squares of polynomials techniques and semidefinite programming, is proposed. As a prototypical example of control of separated flows, the mitigation of the fluctuation kinetic energy in the unsteady two-dimensional wake past a circular cylinder at a Reynolds number equal to 100, via controlled angular motions of the surface, is investigated. A compact control-oriented reduced-order model, resolving the long-term behaviour of the fluid flow and the effects of actuation, is first derived using Proper Orthogonal Decomposition and Galerkin projection. In a full-information setting, linear state-feedback controllers are then designed to reduce the long-time average of the resolved kinetic energy associated to the limit cycle of the system. Controller performance is then assessed in direct numerical simulations.

Key Words: Fluid Flow, Feedback Control, Sum-of-Squares of Polynomials, Semidefinite Programming

1 Introduction

The development of feedback control strategies to manipulate the natural evolution of a fluid flow is one of the key enablers for future advances in efficient transportation, energy generation and distribution, and in many other technologically-relevant industrial sectors. However, despite recent progress in understanding key physical processes and mechanisms in turbulent flows, advances in the ability to effectively control the spatio-temporal evolution in complex geometries have remained more elusive, owing to the nonlinear, multi-scale nature of turbulent motion.

In this paper a novel feedback control design paradigm for fluid flows is introduced, in an effort to address some of the outstanding difficulties. The methodology applies to finite-dimensional, reduced-order, Galerkin-type models of incompressible fluid flows and allows designing polynomial-type state-feedback controllers of arbitrary degree. The nonlinearity of these systems, i.e. a quadratic term which conserves and redistributes energy across the states, can be handled directly. Hence, key nonlinear processes and mechanisms can be taken into account, if not exploited.

The long-term behaviour of the system, crucial to describe the developed state of natural instabilities that arise progressively as the Reynolds number increases, is central in this paradigm, as design targets time averages of a given cost function defined over an infinite horizon. To overcome the objective difficulty of treating long-time averages in nonlinear dynamics, the analysis is shifted to the problems of estimating a bound on the average, rather than considering the average itself, as first proposed in Ref. [1]. The design problem is then recast into determining the controller that reduces/increases the bound, although the reduction/increase of the average itself cannot be formally guaranteed. The bound estimation and optimisation problems are solved by leveraging recent algorithmic advances in Sum-of-Squares of polynomials (SOS) methods and semidefinite programming, [2–4]. These advances have emerged as a promising and numerically tractable basis to solve many computationally hard problems in control for systems whose dynamics are described by polynomial functions, e.g. [5–7]. The application of such methods to various problems in fluid dynamics, from stability analysis to bounds on time averaged quantities, is discussed in Ref. [1].

The mitigation of large-scale velocity fluctuations in the unsteady wake past a circular cylinder at a Reynolds number equal to 100, via controlled angular motions of the surface, is numerically investigated. This flow has established as a paradigmatic benchmark to investigate the dynamics and control of the flow past a bluff-body, as exemplified by the large variety of control strategies that have been proposed, as recently reviewed in Ref. [8].

In section 2 the design paradigm is introduced. The numerical formulation used to solve the governing equations of the fluid flow is then presented in section 3, along with the model order reduction strategy, based on Proper Orthogonal Decomposition and Galerkin projection, [9]. Linear state-feedback controllers are then designed on this control-oriented model and performance is assessed on both the model and in direct numerical simulation of the fluid flow, in a full-information setting. Conclusions are summarised in section 5.

Funding from EPSRC under the grants EP/J011126/1, EP/J010537/1, and EP/J010073/1 and support in kind from Airbus Operation Ltd., ETH Zurich (Automatic Control Laboratory), University of Michigan (Department of Mathematics), and University of California, Santa Barbara (Department of Mechanical Engineering) are gratefully acknowledged.

2 The control design method

2.1 Sum-of-Squares of polynomials

An brief introduction to SOS methods is provided here for the sake of completeness. More details can be found in the cited references. A multivariate polynomial $f(\mathbf{a})$, $\mathbf{a} \in \mathbb{R}^N$ is a SOS, if there exist polynomials $f_1(\mathbf{a}), \cdots, f_m(\mathbf{a})$ such that

$$f(\mathbf{a}) = \sum_{i=1}^{m} f_i^2(\mathbf{a}). \tag{1}$$

If $f(\mathbf{a})$ is a SOS then $f(\mathbf{a}) \geq 0, \forall \mathbf{a}$. In the general multivariate case, however, $f(\mathbf{a}) \geq 0\ \forall \mathbf{a}$ does not necessarily imply that $f(\mathbf{a})$ is SOS. While being stricter, the condition that $f(\mathbf{a})$ is SOS is much more computationally tractable than non-negativity, [4]. At the same time, practical experience indicates that in many cases replacing non-negativity with the SOS property leads to satisfactory results.

2.2 Problem statement

We consider finite-dimensional dynamical systems given as a set of nonlinear, coupled ordinary differential equations, as

$$\frac{\mathrm{d}\mathbf{a}}{\mathrm{d}t} = \mathbf{f}(\mathbf{a}, \gamma) \tag{2}$$

where $\mathbf{f} : \mathbb{R}^N \times \mathbb{R} \to \mathbb{R}^N$ is assumed to be a polynomial function in the state variables vector $\mathbf{a} \in \mathbb{R}^N$ and in the control $\gamma \in \mathbb{R}$, which we assume in this paper to be a single scalar quantity. This is the formulation that arises from Galerkin projection of the governing Navier-Stokes equations for an incompressible flow onto a finite-dimensional orthonormal set of basis functions, [10]. For such systems the vector field $\mathbf{f}$ has linear and quadratic terms, and the latter conserves energy for a large class of boundary conditions of the original equations.

For system (2) it might be of interest to, e.g., reduce the value of some key flow quantity $\Phi(t)$, e.g. drag or energy dissipation rate, referred to as the cost, which we assume can be expressed as a non-negative polynomial function of the state variables and of the control, i.e. $\Phi(t) = \Phi(\mathbf{a}(t), \gamma(t))$. For systems exhibiting turbulent behaviour, long-time statistics of $\Phi(t)$, for example long-time averages,

$$\overline{\Phi} = \lim_{T \to \infty} \frac{1}{T} \int_0^T \Phi(\mathbf{a}(t), \gamma(t)) \mathrm{d}t, \tag{3}$$

are of primary interest, where $\mathbf{a}(t)$ is the solution of (2), with $\gamma = \gamma(t)$ and for some initial condition. Denoting with $\overline{\Phi}^0$ the long-time averaged cost without control, the objective is to design a polynomial-type state-feedback controller of degree d_g

$$\gamma(t) = g(\mathbf{a}(t)), \tag{4}$$

$g : \mathbb{R}^N \to \mathbb{R}$, that manipulates the system (2) such as to reduce the long-time averaged cost to $\overline{\Phi}^*$. We assume at this point that complete information on the instantaneous state of the system is available. Hence, we avoid the necessity of designing an observer which would be required in practical applications, but it is out of the scope of this paper, which focuses on control design only.

Formally, control design is the optimisation problem

$$\overline{\Phi}^* = \begin{cases} \min\limits_{g} \ \overline{\Phi}, \quad \text{s.t.} \\ \dfrac{\mathrm{d}\mathbf{a}}{\mathrm{d}t} = \mathbf{f}(\mathbf{a}, g(\mathbf{a})). \end{cases} \tag{5}$$

The non-convexity of (5), but most importantly the fact that the minimisation of a long-time average is considered, makes its solution rather difficult. The key step is that instead of treating a long-time average directly, we shift the analysis to an upper bound, i.e. a value C for which an algorithm exists proving $\overline{\Phi} \leq C$ for system (2), where the equality holds when the bound is tight. Then, instead of attempting to reduce the long-time average, we reformulate (5) into the problem of designing a controller minimising the upper bound, from C^0, the bound on $\overline{\Phi}^0$, to C^*, the bound on $\overline{\Phi}^*$. This reads as

$$C^* = \begin{cases} \min\limits_{g} \ C, \quad \text{s.t.} \\ \bar{\Phi} \leq C, \ \dfrac{\mathrm{d}\mathbf{a}}{\mathrm{d}t} = \mathbf{f}(\mathbf{a}, g(\mathbf{a})). \end{cases} \tag{6}$$

The hope is that under the action of such a controller, the actual time-average $\overline{\Phi}^*$ will also decrease, although this is not guaranteed to happen in a general case.

2.3 Bounds estimation for uncontrolled dynamics

To derive an upper bound C^0 we introduce a tunable polynomial function in the state variables, $V(\mathbf{a})$, of degree d_V, containing unknown decision variables as its coefficients. Assuming that the trajectories of the system (2) are bounded in some set, the function V and its gradient are also bounded as V is a polynomial. The total time derivative of V along trajectories of the system,

$$\frac{\mathrm{d}V(\mathbf{a})}{\mathrm{d}t} = \frac{\partial V}{\partial \mathbf{a}} \cdot \frac{\mathrm{d}\mathbf{a}}{\mathrm{d}t} = \nabla_{\mathbf{a}} V(\mathbf{a}) \cdot \mathbf{f}(\mathbf{a}), \tag{7}$$

is then also bounded for polynomial $\mathbf{f}$, where $\nabla_{\mathbf{a}} V \triangleq \partial V / \partial \mathbf{a}$ is the gradient of V with respect to the the coordinates of the state space. Then, if a V and a C can be found such that the following polynomial inequality

$$\nabla_{\mathbf{a}} V(\mathbf{a}) \cdot \mathbf{f}(\mathbf{a}) + \Phi(\mathbf{a}) \leq C \tag{8}$$

is satisfied for all $\mathbf{a} \in \mathbb{R}^N$, it can be shown that $\overline{\Phi}^0 \leq C$. This is because the time average of the time derivative contribution vanishes identically under the above assumption of boundedness. Hence, the upper bound C^0 can be obtained by minimizing C over all possible polynomials V of a given degree under the polynomial constraint (8), i.e. by solving

$$\overline{\Phi}^0 \leq C^0 = \begin{cases} \min\limits_{V} \ C \quad \text{s.t.} \\ -\Big(\nabla_{\mathbf{a}} V(\mathbf{a}) \cdot \mathbf{f}(\mathbf{a}) + \Phi(\mathbf{a}) - C \Big) \geq 0 \end{cases} \tag{9}$$

Because constructing a non-negative polynomial is a notoriously difficult problem, we replace the non-negativity constraint in (9) with an SOS constraint, such as to have

$$\overline{\Phi}^0 \leq C^0_{SOS} = \begin{cases} \min\limits_{V} \ C, \quad \text{s.t.} \\ -\Big(\nabla_{\mathbf{a}} V(\mathbf{a}) \cdot \mathbf{f}(\mathbf{a}) + \Phi(\mathbf{a}) - C \Big) \in \Sigma \end{cases} \tag{10}$$

where Σ is the set of all polynomials that have a sum-of-squares decomposition. For a given C, the search for the function V is numerically reformulated into a convex semidefinite programme (SDP) using standard software tools, [12, 13].

The bound estimation is performed by trial-and-error. For a given C we try to find a V satisfying the constraint in (10). If the resulting SOS decomposition satisfies a feasibility-checking condition, see Ref. [14], we decrease C by a δC, and repeat the trial, until such a V cannot be found.

Strengthening the non-negativity constraint to a SOS constraint adds conservativeness in the optimisation, in the sense that, if one were able to solve (9), the upper bound C^0 might be, in principle, lower than the bound C^0_{SOS} found by solving (10), hence the tightness of the obtained bound may not be guaranteed. However, the SOS constraint is numerically tractable, whereas the non-negativity one is not.

2.4 Bounds optimisation for control design

We now consider a tunable polynomial function $V(\mathbf{a})$, and assume initially that the system trajectories will remain bounded under closed-loop control. The optimisation problem equivalent to (10) is now

$$\overline{\Phi}^* \leq C^*_{SOS} = \tag{11}$$
$$\begin{cases} \min\limits_{V,g} \; C \quad \text{s.t.} \\ -\big(\nabla_{\mathbf{a}} V(\mathbf{a}) \cdot \mathbf{f}(\mathbf{a}, g(\mathbf{a})) + \Phi(\mathbf{a}) - C\big) \in \Sigma \end{cases}$$

where the minimisation of the upper bound is now performed over all possible polynomials V and state-feedback polynomial controllers g, for a given degree d_V and d_g, subject to the numerically tractable SOS constraint similarly to (10).

The additional degrees of freedom associated to g can enable a further reduction of the bound, that is $C^*_{SOS} < C^0_{SOS}$. The system is never integrated in time; the bounds C^0 and C^* solely depends on the analytic definition of the vector field $\mathbf{f}$, hence on the structure of the phase space. Because the system's attractors determine the long-term evolution, hence the bound, one can see this design scheme as finding the vector field induced by $g(\mathbf{a})$ that reshapes the attractor of the system such as to reduce favourably the long-time averaged cost.

The bound optimisation problem is non-convex, because one needs to optimise simultaneously the tunable function V and the controller g, and so the tuning variables in V are multiplied with those in g. Hence, the problem is not directly reducible to a semidefinite programme and convex-optimisation-based techniques cannot be readily applied. Alternative iterative algorithms need to be used, e.g. [15] for an overview. The main idea, that we have also used in this paper is: first fix one subset of the decision variables (e.g., that of g in (11)) and solve the resulting linear SDPs in the other decision variables (e.g., correspondingly, that of V in (11)); in the next step, the other decision variables are fixed and the procedure is repeated.

3 Application to a fluid flow

In this section the control design methodology described in section 2 is applied to the problem of mitigating fully-developed vortex shedding, i.e. the nonlinear dynamics of the two-dimensional unsteady wake flow past a circular cylinder at low Reynolds number, $Re = 100$. Flow manipulation is performed by controlling the rotation rate of the cylinder surface.

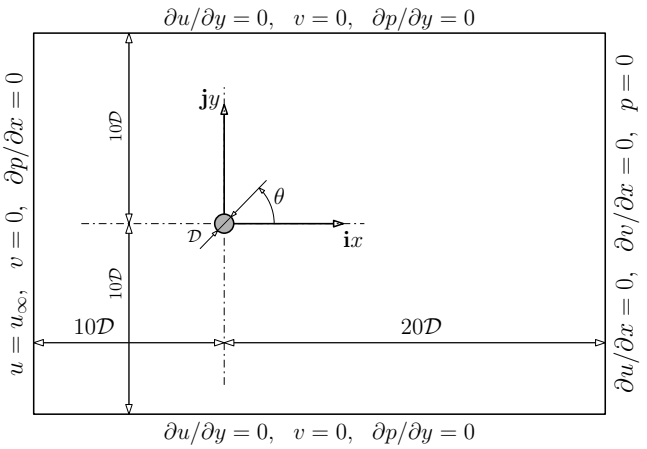

Fig. 1: Schematic of the configuration for the circular cylinder flow, with boundary conditions on the domain boundary.

3.1 Numerical setup

The formulation used to solve the flow problem is based on the Navier-Stokes momentum and continuity equations for a two-dimensional incompressible flow of a viscous fluid

$$\frac{\partial \mathbf{u}}{\partial t} + \mathbf{u} \cdot \nabla \mathbf{u} = -\nabla p + \frac{1}{Re} \nabla^2 \mathbf{u}, \tag{12a}$$
$$\nabla \cdot \mathbf{u} = 0, \tag{12b}$$

where p is the reduced pressure and $\mathbf{u} = u\mathbf{i} + v\mathbf{j}$ is the velocity vector defined on a two-dimensional Cartesian space $\mathbf{x} = x\mathbf{i} + y\mathbf{j}$, centred on the centre of the cylinder, located at $\mathbf{x} = (0, 0)$, and oriented such that the x axis is aligned with the free stream, as sketched in the schematic of figure 1. Normalisation of all variables and of the governing equations, resulting in system (12), is done using the cylinder diameter and the free stream velocity. This yields a definition of the Reynolds number as $Re = u_\infty \mathcal{D}/\nu$, where $\mathcal{D}$ is the cylinder diameters, u_∞ is the free stream velocity and ν is the kinematic viscosity of the fluid.

The Navier-Stokes problem (12) is numerically solved on a triangular unstructured mesh with a finite volume formulation provided by the open source software OpenFOAM, [16]. The computational domain extends for 10 and 20 diameters upstream and downstream of the cylinder, respectively, and spans a total vertical size of 20 diameters. The boundary conditions associated with the problem are also sketched in figure 1. More details can be found in Ref. [17].

In the following we will make use of a standard inner product between vector fields, defined as $\langle \mathbf{v}, \mathbf{w} \rangle = \int_\Omega \mathbf{v} \cdot \mathbf{w} \, \mathrm{d}\Omega$, where Ω is the flow domain.

3.2 Reduced Order Modelling and Proper Orthogonal Decomposition

Spatial discretisation of equation (12), an infinite dimensional system described by partial differential equations (PDEs), leads formally to a finite-dimensional ordinary-differential-equation representation of the dynamics. How-

ever, the extremely large dimension of such a system results in numerically intractable problems, even for moderately complex flows. Model order reduction, whereby the dynamics of a large system are approximated by a model of a handful of degrees of freedom, is used in this paper to allow a numerical solution of the control problem.

We adopt a standard Galerkin projection method, whereby the full dynamics are projected onto a low-dimensional linear subspace, spanned by appropriately selected basis functions, (see [9] for details). To begin with, the velocity vector field is assumed to be approximated by the ansatz

$$\mathbf{u}^N(\mathbf{x},t) = \overline{\mathbf{u}}(\mathbf{x}) + \gamma(t)\mathbf{u}_c(\mathbf{x}) + \sum_{i=1}^{N} a_i(t)\mathbf{u}_i(\mathbf{x}). \quad (13)$$

Here, the full velocity field is decomposed into a solenoidal steady base flow $\overline{\mathbf{u}}(\mathbf{x})$ satisfying homogeneous boundary conditions on the cylinder, a "control flow" $\gamma(t)\mathbf{u}_c(\mathbf{x})$, [18], used to lift the time-dependent inhomogeneous boundary conditions on the oscillating cylinder surface and to include control via the boundary in the dynamic model, and the weighted sum of N solenoidal vector fields $\mathbf{u}_i(\mathbf{x})$, the basis functions, which are assumed to form an orthonormal set. Note that, as a result of this decomposition, the actual control input is γ, i.e. the normalised tangential velocity of the cylinder surface.

In this work we used the snapshot version of Proper Orthogonal Decomposition (POD), [19] to identify the low-dimensional subspace. The motivating observation for the choice of POD in the current context is that when the snapshots used in the POD algorithm are obtained by sampling the system after the developed regime has established, the basis functions describe approximately the axis of inertia of the attractor of the system. This feature is extremely important when modelling the long-term behaviour of the system is of ultimate interest, such as in the present case, where the focus is on the dynamics, (bound estimation), and control, (bound optimisation), of the developed regime.

Our modelling procedure follows closely that of Ref. [11]. With the idea of exciting transient flow structures and obtaining a richer snapshot set, the velocity vector field is sampled from a direct numerical simulation in which the angular motion of the cylinder is driven by an actuation signal with bandwidth mostly around the vortex shedding frequency.

The time-dependent, inhomogeneous boundary conditions on the cylinder are lifted from the snapshots by subtracting, with appropriate amplitude, the control function $\mathbf{u}_c(\mathbf{x})$, a radially-symmetric, hence solenoidal, vector field, with circumferential velocity decaying exponentially with the radius, and with tangential velocity equal to one on the cylinder surface. The arithmetic average of these snapshots, $\overline{\mathbf{u}}(\mathbf{x})$, is removed before applying the POD algorithm and it is used as the base flow in (13).

As a compromise between computational cost and model accuracy, we selected the first $N = 9$ POD modes, capturing about 91% of the total fluctuation kinetic energy in the snapshots. In addition, this model is augmented with a shift mode, [20], a particular mode spanning the direction from the steady base flow to the unstable, steady and symmetric solution of (12).

Standard Galerkin projection is then performed by inserting the expansion (13) in (12), and setting the inner product with each of the modes in turn to zero. Neglecting the small contribution arising from the projection onto the pressure gradient field, as commonly done for this fluid flow, e.g. [11, 20], results in the nonlinear system of first-order coupled ordinary differential equations, the reduced-order model (ROM):

$$\begin{aligned}\frac{\mathrm{d}a_i}{\mathrm{d}t} &= c_i + \sum_{j=1}^{N} L_{ij}a_j + \sum_{j=1}^{N}\sum_{k=j}^{N} Q_{ijk}a_j a_k + m_i\frac{\mathrm{d}\gamma}{\mathrm{d}t} \\ &\quad + e_i\gamma + b_i\gamma^2 + \sum_{j=1}^{N} F_{ij}a_j\gamma,\ i = 1,\dots N, \quad (14)\end{aligned}$$

where $\gamma \in \mathbb{R}$ is the control input, and $\mathbf{a} \in \mathbb{R}^{10}$ is the state vector as in equation (2). Definitions of the coefficients $c_i, L_{ij}, Q_{ijk}, m_i, e_i, b_i, F_{ij}$ arising from the projection can be found, for example, in Ref. [21]. Numerical time integration of the ROM is performed using a fourth-order Runge-Kutta scheme with time step equal to 10^{-3}.

The ten-mode reduced-order model obtained directly from Galerkin projection is able to represent the dynamics of the full-order system only over a short time scale, i.e. about one shedding cycle, and the long-term behaviour is not correctly represented. Furthermore, poor controllability of this compact model was observed. As a result, a model calibration scheme, following the work in Ref. [21], has been used to ensure correct tracking of the uncontrolled limit cycle and a better input-output behaviour.

3.3 Cost function

Similarly to previous works, [11, 22], in the present paper the cost function to be reduced is the domain integral of the turbulent kinetic energy of the velocity fluctuations resolved by the ansatz (13), plus a penalisation on the control, i.e. the quantity

$$\Phi(\mathbf{a}(t)) = \frac{1}{2}\mathbf{a}(t)^T\mathbf{a}(t) + R\gamma^2(\mathbf{a}(t)). \quad (15)$$

The penalisation factor R does not have an immediate physical meaning, but it is used as a design parameter as a means to artificially limit the amplitude of the control.

4 Results

The long-time averaged cost (15) was calculated from long numerical integrations of the ROM without control, starting from several random initial conditions. All trajectories converged to the same stable limit cycle and the associated long-time averaged cost was $\overline{\Phi}^0 = 3.07$.

Linear state-feedback controllers, i.e. $d_g = 1$, have been then calculated, for $d_V = 4$, and for different penalisation factors R. Tests for $d_V = 6$ showed no difference, as all bounds are tight to the actual average from simulation with $d_V = 4$. For linear controllers, of the form $\gamma(t) = \sum_{i=1}^{N} k_i a_i(t)$, it is possible to get rid of the term $m_i\mathrm{d}\gamma/\mathrm{d}t$ in (14), by noting that $\mathrm{d}\gamma/\mathrm{d}t = \sum_{i=1}^{N} k_i \mathrm{d}a_i/\mathrm{d}t$

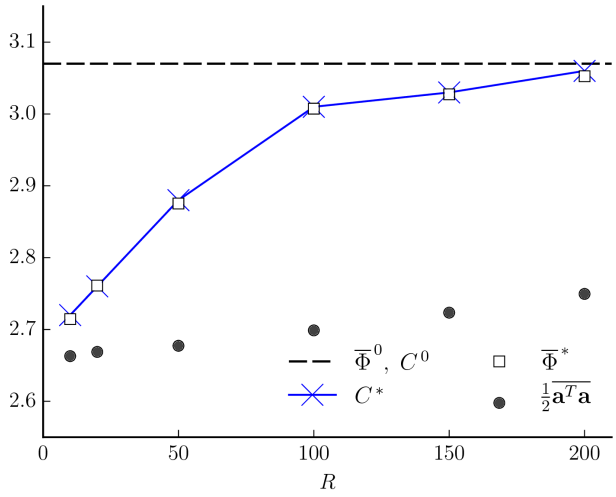

Fig. 2: Performance of linear feedback controllers as a function of the penalisation factor R in closed-loop simulation of the ROM. Blue line and crosses ($\times$): upper bound of the long-time averaged cost; open squares ($\square$): long-time averaged cost from simulation of the ROM; closed circles ($\bullet$): long-time average of the resolved fluctuation kinetic energy. The horizontal line denotes the time average/upper bound for the uncontrolled system.

and using the state equation to get

$$\mathrm{d}\gamma/\mathrm{d}t = \frac{1}{1 - \times \sum_{l=1}^{N} k_l m_l} \sum_{i=1}^{N} k_i \qquad (16)$$
$$\times \Big(c_i + L_{ij} a_j + Q_{ijk} a_j a_k + e_i \gamma + b_i \gamma^2 + F_{ij} a_j \gamma \Big),$$

which is the plugged back in the state equation (14). For nonlinear controllers, another approach is necessary, as the denominator in (16) would contain an expression in the state variables, making the resulting system non-polynomial in the state variables. Nevertheless, it is worth pointing out that even though the feedback is a linear function of the state, the nonlinear dynamics of the ROM are completely taken into account in the design.

4.1 Feedback control on ROM

In figure 2 the control performance in closed-loop simulation of the ROM is summarised. Long-time averages of the cost are computed from numerical simulations started from an initial condition on the ROM's limit cycle and by discarding initial transients as control is activated. The figure reports the upper bound C^*, (blue line and crosses), the actual time average $\overline{\Phi}^*$ from simulation, (open squares), and the long-time average of the resolved fluctuation kinetic energy $\mathbf{a}^T\mathbf{a}/2$, (closed circles), with the difference between the two latter quantities being the average cost of control. The horizontal line is the upper bound for the uncontrolled system, which is tight to the actual time average from numerical integration of the ROM. Control design successfully reduces the upper bound. The reduction is larger for small R, as larger control magnitudes are allowed. The maximum reduction of the bound is relatively small, i.e. about 6% for $R = 50$; larger reduction can be found for smaller penalisation factors, although these controllers performed poorly in DNS. Interestingly, a significant part of the total time averaged cost comes, artificially, from the control penalisation, especially at large values of R.

4.2 Feedback control in DNS

In direct numerical simulation, at the beginning of the k-th time step at time t_k, the current system state is obtained by projecting the POD modes on the current fluctuating velocity field as

$$a_i(t_k) = \langle \mathbf{u}_i(\mathbf{x}), \mathbf{u}(\mathbf{x}, t_k) - \overline{\mathbf{u}}(\mathbf{x}) - \gamma(t_{k-1})\mathbf{u}_c(\mathbf{x}) \rangle. \quad (17)$$

The new control action $\gamma(t_k)$ is calculated and it is kept constant along the time step $t_{k+1} - t_k$, in a zero-order hold fashion.

Controller effectiveness in direct numerical simulation is reported here in terms of the total power coefficient, a physically meaningful quantity that expresses the normalised total power spent to sustain the motion of the cylinder, [23]. It is the sum of the power $P_D = Du_\infty$ spent to move the cylinder at velocity u_∞ against the drag force D and the control power $P_M = M\dot{\theta}$ required to rotate the cylinder at angular speed $\dot{\theta}$, against the viscous torque M exerted by the fluid on the cylinder.

The normalised total power coefficient reads as

$$C_P = \frac{P_D + P_M}{1/2\rho u_\infty^3 \mathcal{D}} = C_D + 2C_M\gamma, \qquad (18)$$

where C_D and C_M are the coefficients of drag and moment, and γ is the normalised surface velocity as introduced above. All actions on the body are computed by appropriate integration of the pressure and viscous forces around the cylinder surface, and are expressed per unit span.

Time histories of the total power coefficient obtained from direct numerical simulation of the closed-loop system, are reported in figure 3, for $R = 100$, top panel, and $R = 150$, bottom panel, with red dashed lines. The drag coefficient C_D, which does not include the control power, is also reported as a black solid line. The difference between the two, i.e. $C_P - C_D$, is the normalised energy per unit time and unit span required to actively control the flow.

For $R = 150$, the SOS controller successfully reduces both the total power and drag coefficients. Analyses not reported here show that the both the kinetic energy of the velocity fluctuations resolved by the ansatz (13) as well as the total fluctuation kinetic energy are reduced by about 8%. Physically, control mitigates vortex shedding by interfering with the periodic generation and shedding of vortical structures in the near wake, resulting in a restructuring of the entire wake flow. The time averaged percentage drag reduction, normalised with the drag coefficient of the uncontrolled flow, is 4.6% for this case. This value is not as high as in previous control studies on this same configuration. Using optimal control theory, drag reductions of 7% at $Re = 75$ and 15% at $Re = 150$, were achieved in [24]. However, these authors used the Navier-Stokes equations directly for control design in a predictive setting, and not a reduction thereof.

Interestingly, the long-term cost of the control is extremely small, with peaks of $C_P - C_D$ not exceeding 0.002.

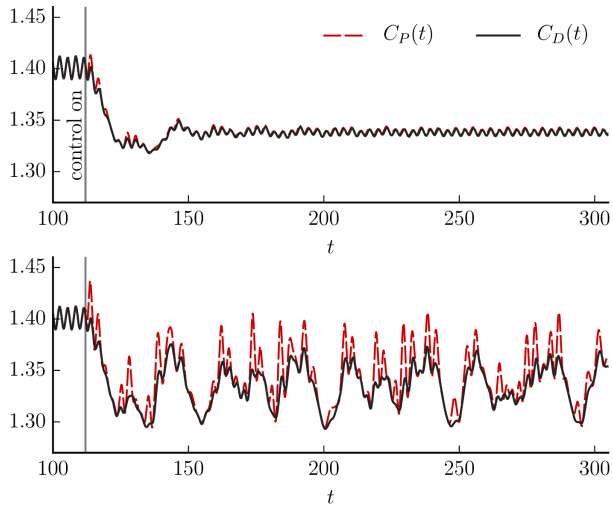

Fig. 3: Time histories of the total power and drag coefficients, $C_P(t)$ and $C_D(t)$, obtained from closed-loop direct direct numerical simulations, for $R = 150$, top panel, and $R = 100$, bottom panel.

Thus, the control strategy identified is very efficient. Following [24], the control efficiency can be quantified by the power saving ratio $\mathrm{PSR} = (\overline{C_P}^0 - \overline{C_P}^*)/2\overline{C_M\gamma}^*$, i.e. the ratio between the power saved and the power spent for control, in a time-averaged sense. The PSR is remarkably large, and equal to about 75 for $R = 150$. For comparison, in Ref. [24], the authors obtained a PSR equal to 51 at $Re = 150$, and 122 at $Re = 75$.

For $R = 100$, in the initial stages after activation of control, the drag and power coefficients decrease significantly. The drag minima can be as low as 1.30, suggesting that the control design methodology is indeed effective. The drag coefficient associated with the steady laminar solution is, in our setup, 1.14. As a result, the drag coefficient reduction, compared to the drag associated to vortex shedding, [24], can be instantaneously as large as 38%. Nevertheless, performance is quickly lost after about 30 time units, and both quantities exhibits a characteristic low-frequency periodic variation, with C_P showing large spikes due to large control activity. Further analyses of the flow dynamics show that such a loss of performance is associated to an instability of the controlled wake that the ROM, hence the control design, is not able to describe.

5 Discussion and conclusions

The main contribution of the present paper is the development of a novel feedback control design paradigm for Galerkin-type models of incompressible fluid flows.

From an algorithmic perspective, this paradigm is grounded on computationally efficient approaches to construct positive polynomial functions, commonly known as Sum-of-Squares methods, that recast the search to the formulation and solution of semidefinite programmes.

The key distinguishing features are that i) the long-term behaviour of the system is central in the design, as long-time averages of key flow quantities can be optimised by control design, and that ii) the nonlinearity of turbulent fluid flows, responsible of key physical processes, is taken directly into account in the design process.

As a benchmark, the problem of mitigating the kinetic energy of velocity fluctuations in the unsteady wake of a circular cylinder at $Re = 100$, via controlled rotary motions of the surface, in a full-information state feedback arrangement, has been investigated. A compact POD-Galerkin reduced-order model of the actuated wake flow was first derived. Linear state-feedback controllers were then derived. The feedback system was energetically efficient, as the maximum power saved per unit control power spent was around 75. For low values of the penalisation factor, the greater control input resulted in better performance just after activation of control, but eventually performance worsened significantly. This is not a limitation of the present design method, but is it rather driven by the POD-Galerkin modelling strategy used, which is known to lack robustness to actuation. We expect that improvements in the modelling strategy will result in increased performance in direct numerical simulation.

References

[1] Chernyshenko, S. I., Goulart, P., Huang, D. & Papachristodoulou, A. 2014 Polynomial sum of squares in fluid dynamics: a review with a look ahead. *Philosophical Transactions of the Royal Society of London A: Mathematical, Physical and Engineering Sciences* **372** (2020).

[2] Huang, D., Chernyshenko, S., Goulart, P., Lasagna, D., Tutty, O. & Fuentes, F. 2015 Sum-of-squares of polynomials approach to nonlinear stability of fluid flows: an example of application. *Proceedings of the Royal Society A* **471**: 20150622.

[3] Papachristodoulou, A. & Prajna, S. 2002 On the construction of Lyapunov functions using the sum of squares decomposition. In *Decision and Control, 2002, Proceedings of the 41st IEEE Conference on*, , vol. 3, pp. 3482–3487. IEEE.

[4] Parrilo, P.A. 2003 Semidefinite programming relaxations for semialgebraic problems. *Mathematical programming* **96** (2), 293–320.

[5] Nguang, S.K., Krug, M. & Saat, S. 2011 Nonlinear static output feedback controller design for uncertain polynomial systems: an iterative sums of squares approach. In *Proceedings of the IEEE Conference on Industrial Electonics and Applications, 2011*, , vol. 3, pp. 979–984. IEEE.

[6] Valmorbida, G., Tarbouriech, S. & Garcia, G. 2013 Design of polynomial control laws for polynomial systems subject to actuator saturation. *IEEE Transactions on Automatic Control* **58** (7), 1758–1770.

[7] Zhao, D. & Wang, J.L. 2010 Robust static output feedback design for polynomial nonlinear systems. *International Journal of Robust and Nonlinear Control* **20**, 1637–1654.

[8] Choi, H., Jeon, W. & Kim, J. 2008 Control of flow over a bluff body. *Annu. Rev. Fluid Mech.* **40** (1), 113–139.

[9] Holmes, P., Lumley, J. & Berkooz, G. 1998 *Turbulence, Coherent Structures, Dynamical Systems and Symmetry*. Cambridge University Press.

[10] Fletcher, C.A.J. 1984 Computational Galerkin methods. In *Computational Galerkin Methods*, pp. 72–85. Springer Berlin Heidelberg.

[11] Bergmann, M., Cordier, L. & Brancher, J.P. 2005 Optimal rotary control of the cylinder wake using Proper Orthogonal Decomposition reduced-order model. *Physics of Fluids (1994-present)* **17** (9), 097101.

[12] Löfberg, J. 2004 Yalmip : A toolbox for modelling and optimization in MATLAB. In *Proceedings of the CACSD Confer-*

ence. Taipei, Taiwan.

[13] Prajna, S., Papachristodoulou, A., Seiler, P. & Parrilo, P. A. 2004 *SOSTOOLS: Sum of squares optimization toolbox for MATLAB*.

[14] Löfberg, J 2009 Pre- and Post-Processing Sum-of-Squares programs in practice. *IEEE Trans. Automat. Contr.* **54** (5), 1007–1011.

[15] Henrion, D. & Garulli, A. 2005 *Positive polynomials in control*, , vol. 312. Springer Science & Business Media.

[16] Jasak, H., Jemcov, A. & Tukovic, Z. 2007 Openfoam: A C++ library for complex physics simulations. In *International workshop on coupled methods in numerical dynamics*, , vol. 1000, pp. 1–20.

[17] Lasagna, D. & Tutty, O. 2015 Wall-based reduced order modelling. *International Journal of Numerical Methods in Fluids* DOI: 10.1002/fld.4163.

[18] Kasnakoğlu, C., Serrani, A. & Efe, M. 2008 Control input separation by actuation mode expansion for flow control problems. *Int. J. Control* **81** (9), 1475–1492.

[19] Sirovich, L. 1987 Turbulence and the dynamics of coherent structures. Part I: Coherent structures. *Quart. Appl. Math.* **45** (3), 561–571.

[20] Noack, B.R., Afanasiev, K., Morzynski, M., Tadmor, G. & Thiele, F. 2003 A hierarchy of low-dimensional models for the transient and post-transient cylinder wake. *Journal of Fluid Mechanics* **497**, 335–363.

[21] Cordier, L., Majd, E., Abou, B. & Favier, J. 2010 Calibration of POD reduced-order models using Tikhonov regularization. *International Journal for Numerical Methods in Fluids* **63** (2), 269–296.

[22] Graham, W.R., Peraire, J. & Tang, K.Y. 1999 Optimal control of vortex shedding using low-order models. Part II: model-based control. *International journal for numerical methods in engineering* **44** (7), 973–990.

[23] Bergmann, M., Cordier, L. & Brancher, J.P. 2006 On the power required to control the circular cylinder wake by rotary oscillations. *Phys. Fluids* **18** (8), 088103.

[24] Protas, B. & Styczek, A. 2002 Optimal rotary control of the cylinder wake in the laminar regime. *Physics of Fluids (1994-present)* **14** (7), 2073–2087.